CALCULATION OF PRESSURE FIELD IN THE PROBLEM OF SONIC BOOM FROM VARIOUS THIN AXISYMMETRIC BODIES

A.V. Potapkin, D.Yu. Moskvichev

Khristianovich Institute of Theoretical and Applied Mechanics SB RAS
630090, Novosibirsk, Russia

When solving the problem about the sonic boom from the body in supersonic flight one should consider several factors. Such factors are body shape, flight line and flight conditions, atmosphere state, ground forms under the flight line. An example of such a problem is that one about sonic boom minimizing. By now various methods to determine the shock waves and pressure fields parameters under the flight line were elaborated. Many results were obtained by means of these methods. The following classification can be suggested: experimental, analytical and numerical methods, as well as the combined ones. The experimental methods comprise full-scale experiments, and ones in ballistic tracks and wind tunnels. The direct calculation of the flow parameters in the far field is possible when applying analytical methods. The numerical methods of calculating the flow on fixed or moving difference grids related to the shock waves system. The most perspective are the combined methods for determining flow parameters applying the following steps:

1. analytical calculations of near field parameters with further numerical calculation of flow in the far field,
2. experimental determination of the near field flow parameters with further parameters extrapolation in the far field by the analytical methods,
3. numerical calculation of the near flow field with further analytical extrapolation of the solution in the far field,
4. numerical calculation of the near flow field on fixed difference grids with further numerical calculation of the far flow field in the moving difference grids.

The method 1 efficiency is demonstrated solving the problem about sonic boom in case of non-steady supersonic body flight [1]. The method 2 was applied in the work [2] for recalculating the experimental data in the far field. An example of method 3 application can be the way to solve the problem about optimizing body shape to minimize the sonic boom [3]. The possibilities of the method 4 are demonstrated in the work [4] by the example of the test problems about the sonic boom from the thin axisymmetric body. The work [5] illustrates the development and complication of the methods combined. This work suggested the "phantom bodies" method as developing the method 3 to find the parameters of the sonic boom in case of three-dimensional sources of the shock waves.

A result showing the body shape influence on the sonic boom level is known in the problem about minimizing the sonic boom. The work [6] showed that the thin pointed axisymmetric bodies with minimal wave drag form lower sonic boom in the far field. If one introduces an additional factor in this problem, specifically the state of atmosphere (for example changing of atmosphere near the body by means of energy supply), then this conclusion might be wrong.

The present work represents the calculation results of the pressure fields in the problem about the sonic boom from various axisymmetric thin bodies. The calculations were done applying the improved combined method 3. The numerical calculations of the near and far fields were done by two models, especially one used the model of viscous heat-conducting gas and the heat-conductive non-viscous ideal one. Two-dimensional non-steady Navier-Stokes equations were used. They were complemented by the turbulence model S–A (Spalart – Allmaras model) and two-dimension non-steady Euler equations. When calculating the near and far field we used the commercial software

ANSYS Fluent (second order approximation scheme). The stationary solution was found by the relaxation method. The calculations of the far field allowed finding out the body shape influence and the state of atmosphere near the body on the shock parameters.

The far field was calculated by means of the "phantom bodies" method. This method suggests successive calculation of the near and far flow field. The general scheme is shown in Fig. 1. The parameters of the near field *2* were used to build the "phantom body". The "phantom body" is set by the digital string of the points *3* on the flight line where the Whitham [7] function values and longitudinal points coordinates were calculated by the parameters of the near field. In such a manner the initial body shape was substituted by the "phantom body" system, for which the calculation of the far field according to the Whitham theory was done. The algorithm suggested allowed calculating the pressure profile in the far field *4* in the selected meridional plane. The spatial pattern of the flow is obtained when calculating in several meridional planes. In such a case in each meridional plane the initial shock waves sources are substituted by the appropriate "phantom bodies" and the far field flow is calculated independently in every plane. Using the "phantom bodies" allows reducing the dimension of the problem to be solved and calculating the far field of the three-dimensional flow by the Whitham theory with obvious emphasizing of the shock waves front.

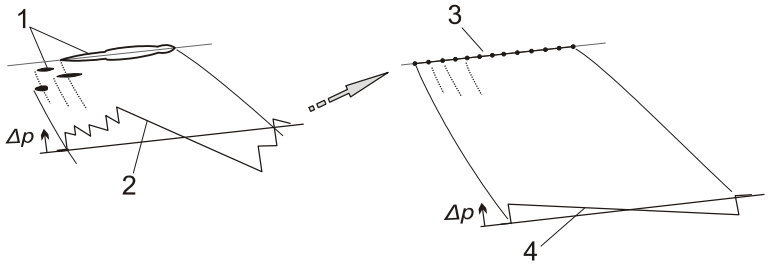

Fig. 1. The scheme of "phantom bodies" method application.
1 – shock waves source, *2* – excessive pressure profile in the near field, *3* – "phantom body", *4* – excessive pressure profile in the far field.

The realization of "phantom body" algorithm building and the calculation of the far field parameters in the selected meridional plane is shown in Fig. 2. The "phantom body" longitudinal coordinates l_1, l_2…l_n and the Whitham function F_1, F_2…F_n were calculated by the excessive pressure profile selected *4*. Calculating the "phantom body" longitudinal coordinates was done by means of geometrical acoustics linear relations. To set univalently the "phantom body" characteristics values one suggested the body thickness equal to zero. As usual, this does not insert any important errors into the calculation results. The appropriate values of the Whitham function $F_i = F(l_i)$ were calculated by known values ΔP_i in the excessive pressure profile points *4*. After F_i was calculated

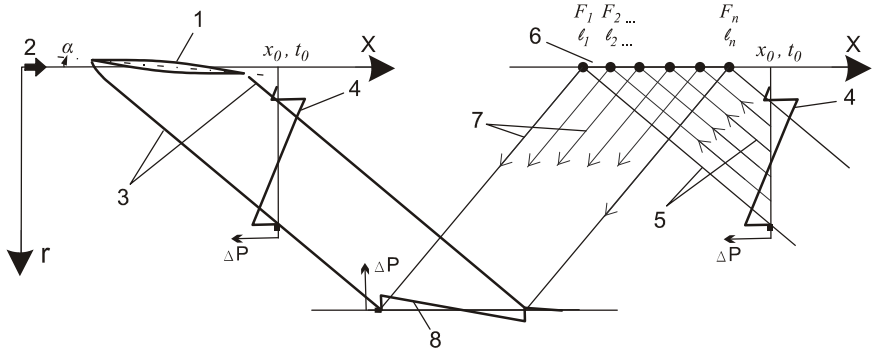

Fig. 2. Building the "phantom body" and calculating the far field in the meridional section selected.
α – angle of attack; x_0,t_0 –distance from the body nose and the moment of time accordingly, for which the excessive pressure profile in the far field was selected. *1* – body, *2* – windstream direction, *3* – bow and closing shocks in the flow field, *4* – excessive pressure profile in the near field, *5* – linear characteristics, *6* –"phantom body", *7* – acoustic beams, *8* – excessive pressure profile in the far field.

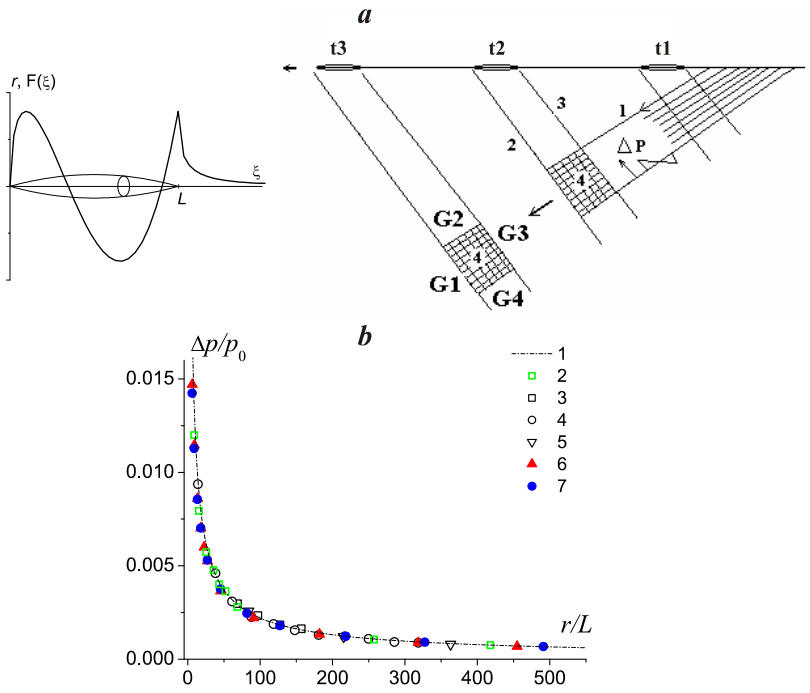

Fig. 3. Calculations of head shock wave intensity in the far field form thin axisymmetric body [4, 5].

a: Axisymmetric body, the Whitham function and the scheme of 2D calculations in the moving grids; *L* – body length, *r* – radial coordinate, *ξ* – characteristic, *F(ξ)* – Whitham function, *t1*, *t2*, *t3* – are successive instants of time, *G1*, *G2*, *G3*, *G4* – the boundaries of moving difference grid. *1* – acoustic beams, *2*, *3* – head and tail shock waves, *4* – moving difference grid;
b: Calculation results of head shock wave intensity in the far field; *1* – asymptotic law $\Delta P/P_0 \sim (r/L)^{-3/4}$; *2* – calculation by the Whitham theory; *3, 4, 5* – the calculation results of the far field in moving difference grids [4]; *6, 7* – head wave intensity calculations by the "phantom bodies" method[5].

the excessive pressure profile *8* was determined in the far field. The excessive pressure profile was built by means of nonlinear relations that results by non-uniqueness of the solution. This non-uniqueness was eliminated in accordance with the Landau rule for determining the position of shock waves [8] by means of excessive pressure function [9].

The "phantom bodies" method was tested in the calculations of parameters of the shock wave from thin axisymmetric and space-form bodies [4, 5]; and it was used in the calculations of the far field parameters in the problems with several shock waves sources. The axisymmetric body with relative thickness in the midsection 10%, the Whitham function and the scheme of the far field calculation in the moving difference grids are shown in Fig. 3*a*. The far field calculation is based on the numerical solution of the 2D non-stationary Euler equations in the moving difference grids related to the system of selected shock waves. The 2D non-stationary gas-dynamic equations were solved in the cylindrical coordinate system. The body position on the flight line at various moments of time was shown. An area *4* was selected for a moment of time *t2* near the body. The area *4* is limited by the moving boundaries *G1*, *G2*, *G3* and *G4*. The flow parameters in the area 4 were accepted as initial data for the calculation of the far field by the method of S.K. Godunov [10] in the moving difference grid. Figure 3*b* represents the calculation results done for the windstream with the Mach number 2.4. It shows the results of calculations done by means of the Whitham theory, the calculation results in moving difference grids and the results obtained by the "phantom bodies" method. The comparison of the results shows that the solution in the far field obtained by two-dimensional Euler equations differs from the Whitham solution not more than 2% to the distances *r/L*~400 (*L* – body length). The solutions obtained by the "phantom bodies" method agrees with the solutions in the moving difference grids.

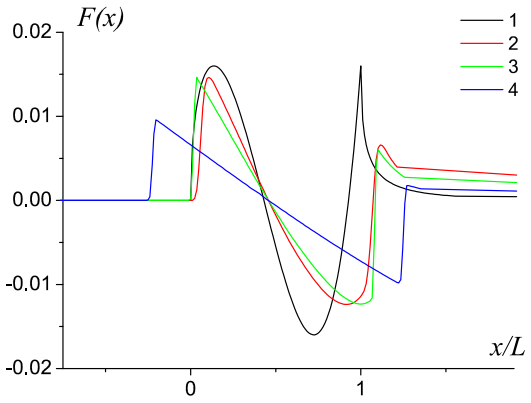

Fig.. 4 The Whitham function for axisymmetric body and "phantom" bodies build in accordance with the pressure profiles.
1 – Whitham theory; *2* – x_0/L = 2.5; *3* – x_0/L = 5; *4* – x_0/L = 45.

Figure 4 shows the "phantom bodies" method application in the sonic boom calculations. The line *1* in the figure shows the Whitham function obtained by the Whitham theory for the same axisymmetric body at the Mach number of the windstream equal to 2. The lines *2–4* show the Whitham function calculated for the "phantom" bodies. The near and mean flow field is calculated by the viscous gas model. The lines *2* and *3* coincide well between each other. The errors when building the "phantom" body by means of the linear theory at Whitham function recovery for long distances x_0/L can be seen at comparisons of the lines *2*, *3* and *4*. The recovered "phantom" body Whitham function for $x_0/L = 45$ differs significantly from the solutions for low x_0/L. The reason of this difference is that the linear theory does not consider the change of the wave length in dependence of the distance. The calculations of the head shock wave intensity in the far field ($r/L \sim 500$) done by means of the Whitham function shown by the lines *1*, *2* and *3* differ from each other for not more than 5%. The head wave intensity calculated from the distance $x_0/L = 45$ (line *4*) differs from the Whitham solution for 12%.

The near field flow calculations by the models of non-viscous and viscous gas are shown in Fig. 5. The isolines of gas density near the body are shown. The concentration of isolines shows the position of head and tails shock waves. Considering the gas viscosity in the calculations allows seeing formation of the boundary layer on the body surface and of the trace behind the body. In such a case the tails shock wave appears as hanging shock.

Figure 6 represents the pressure profiles for two distances from the body nose. The line *1* shows the calculations with non-viscous gas, the line *2* shows the calculations considering the viscosity. One can see the difference for $x_0/L = 1.5$ in the position and intensity of tail shock in calculations with non-viscous and viscous gas. The solutions in the area between the head and tails shocks coincides (Fig. 6*a*) When moving apart from the body (Fig. 6*b*) the solution for non-viscous and viscous gas coincide.

These results shows that when calculating the sonic boom from the thin bodies with smooth generatrix one may not consider the gas viscosity. At the same time this conclusion can not be propagated to axisymmetric bodies of other shape and for three-dimensional ones as well. When flowing such bodies a system of intermediate shocks can be formed; calculation of their intensity depends on the gas model selected. The intermediate shocks can joins the head shock wave and influence the results of sonic boom calculations in the far field.

The calculations results by means of "phantom bodies" method are represented below. These results were obtained for various thin axisymmetric bodies for windstream Mach number equal to 2. The calculations were done for five various axisymmetric bodies. All the bodies had the same

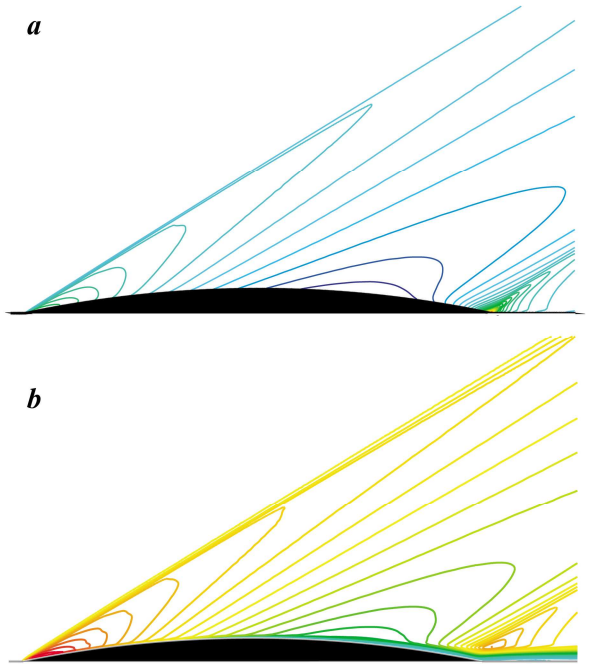

Fig. 5. Density fields calculated by the models of non-viscous (*a*) and viscous (*b*) gas for a axisymmetric body.

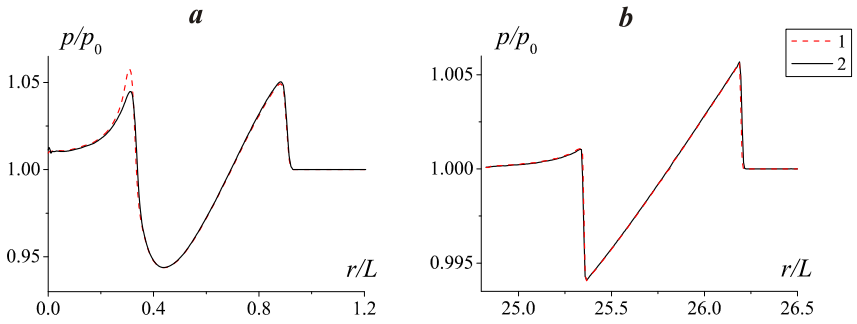

Fig. 6. Pressure profiles in the calculations by the non-viscous and viscous gases.
a – $x_0/L \sim 1.5$, b – $x_0/L \sim 45$.
1 – non-viscous gas, *2* – visous gas.

length L and the same diameter D in the midsection with relative thickness 10 %. The bodies generatrix are shown in Fig. 7. To see the difference between the surface shape of the thin bodies the coordinate axes have different scale in Fig. 7. The body generatrix N1was set by the formula $r = 0.2 \times (x - x^2)$, where r is radial coordinate of the body surface generatrix, $0 \le x \le L$ is distance from the body nose along the body axis. The body N5 represents two conjugate cones. The surface shapes of the bodies N2, N3, N4 are intermediate between the shapes of the bodies N1 and N5.

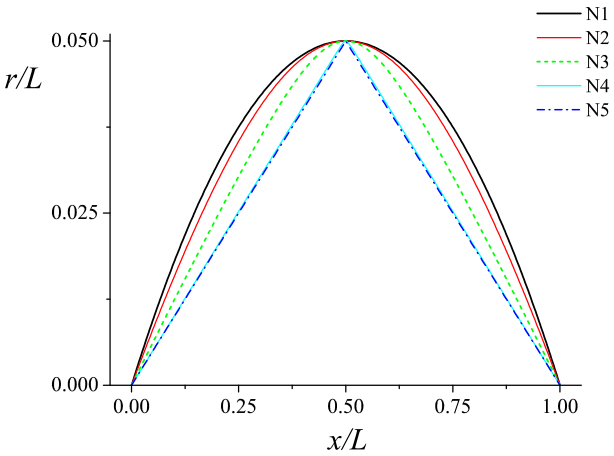

Fig. 7. Axisymmetric bodies generatrix.

Figure 8 shows the pressure profiles calculated by the viscous gas model for the bodies of different shape. The profiles are shown for fixed distances from the body nose (x_0/L = const). Figure 8*a* shows the profiles for x_0/L = 2.5, and Fig. 8*b* shows the pressure profiles for x_0/L = 30.

The head shock wave intensity for $x_0/L \sim 2.5$ from the body N5 is ~ 8% lower than for the body N1. At the same time a compression wave can be seen at the pressure profile behind the bow shock. When moving apart from the body ($x_0/L \sim 30$) the intensity of head shock wave from the body N5 arises thanks to the compression wave and becomes greater than the intensity of the shock wave from the body N1. The calculations of head wave intensity in the far field are shown in Fig. 9. The calculations results for the bodies N1, N2, N3, N5 are represented and the asymptotic law built by the Whitham solution for the body N1 $\Delta p/p_0 \sim (r/L)^{-3/4}$ is shown.

In the far field the shock wave intensity from the body N5 is 5% grater than the values of the intensity values of the wave from the body N1 and it overcomes the Whitham asymptotic nearly for

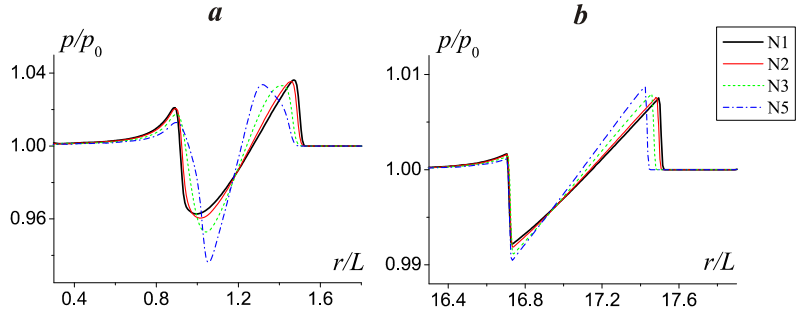

Fig. 8. Pressure profiles (viscous gas) for the bodies of various shape in the near and far fields.
a – $x_0/L \sim 2.5$, b – $x_0/L \sim 30$

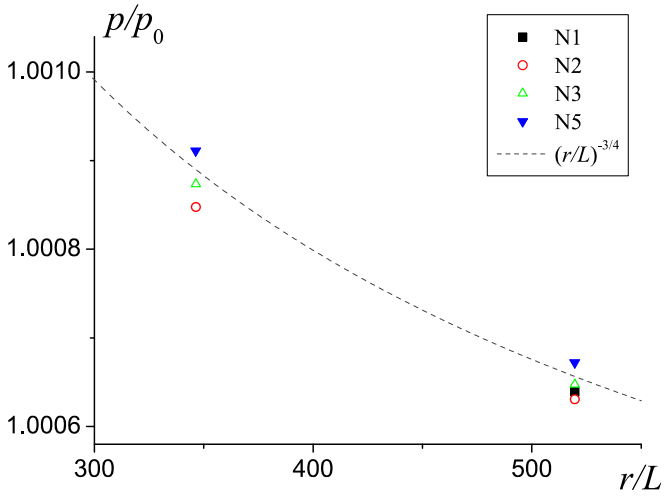

Fig. 9. Calculation of head shock wave intensity in the far field.

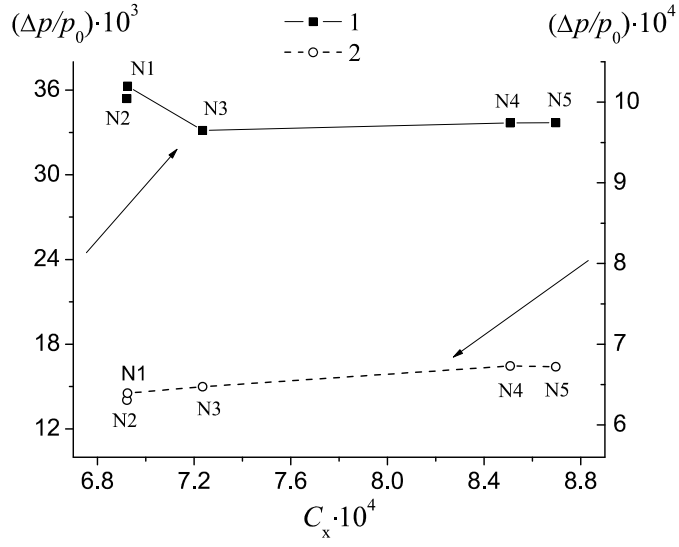

Fig. 10. Intensity of the head shock wave dependence on the drag coefficient for thin bodies of various shape. *1* – $r/L \sim 1.5$, *2* – $r/L \sim 520$.

2.5%. Figure 10 shows the intensity of the head shock wave as the function of dimensionless waves drag coefficient for the bodies with various shape at different distances from the bodies. The line *1* shows the intensity of head shock wave at the distance of $r/L \sim 1.5$, the line *2* shows the intensity of the head wave at the distance $r/L \sim 520$. The form of the curve 2 correlates with the result known [6] about the lowest sonic boom from thin pointed bodies having the lowest wave drag in the homogeneous stream. The points N1-N5 correspond to the bodies of different shape (see Fig. 7). Te highest wave drag coefficient for which one can observe the maximum level of sonic boom in the far field.

The energy supply to the gas near the body causes the formation of local inhomogeneities in the windstream. Figure 11 shows the gas density field near the body N1. The concentration of isolines shows the position of shock waves and the thermal wake frontier from the source of heat. The source of heat is torus shaped with a body inside. The heat of source was placed at the distance $x/L = 0.4$ from the body nose downstream. The distance from the torus circle generatrix center to the axis of symmetry $r/L = 0.3$, the torus circle radius $r_0/L = 0.05$.

The source of heat is in front of the head shock wave from the body and results by forming the system of shock and rarefaction waves. In the cases when the shock wave from the source of heat is weaker than the head shock one from the body. The head shock wave gets up to the wave from the source and joins it. One can see well in the figure that the change of the shock waves angle of slope from the body when passing through the thermal wake and the deformation of the thermal wake when interacting with the discharging waves. The shock wave from the source is reflected by the shock wave from the body surface behind the mid section. The flow separation is formed behind the shock wave reflected from the body on it surface, which causes the reduce of wave drag of the body pressure profiles in the near and mean fields are showed in Fig. 12. We showed the results of pressure calculations of pressure obtained at various energy supply for two distances from the body nose $x_0/L \sim 5$ и $x_0/L \sim 30$.

The line *1* shows the pressure profile at zero energy supply (the body N1, homogeneous external flow), the lines *2* and *3* show the pressure

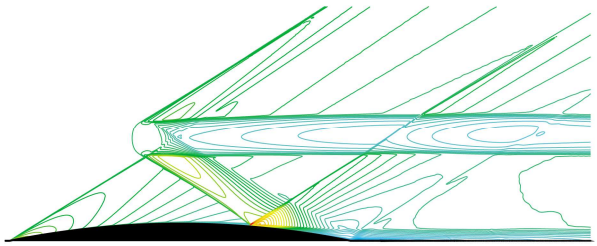

Fig. 11. Gas density isolines when the heat is supplied close to the body.

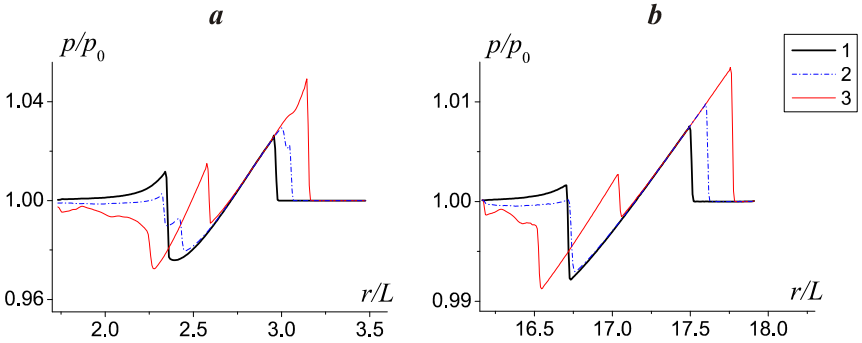

Fig. 12. Pressure profiles in the near and mean flow field for the body N1 in case when the heat source is located close to the body.

a – x_0/L = 5, *b*– x_0/L = 30.

1 – T/T_0 = 1, *2* – T/T_0 = 1.123, *3* – T/T_0 = 1.4.

profiles at T/T_0 = 1.123 и T/T_0 = 1.4 . Here: T is gas temperature inside the heat source, T_0 is temperature of the windstream (T_0 = 300 K).

On can see on the profiles the position and intensity of the shock waves from the heat source, head shock wave from the body and the shock wave reflected from the shock wave body. The pressure profile *2* shows that the head shock wave from the body is much powerful than the shock wave from the source of heat. The shock wave from the body reaches the wave from the source and enhances it. The tail shock wave from the body decreases coming through the thermal wake and comes up the wave reflected from the body. The head wave from the body is weaker than the wave from the heat source on the profile *3*. The wave reflected from the body on the pressure profile looks like an intermediate shock. The tail shock wave from the body becomes weaker and a trace in the form of compression wave is formed behind it.

Figure 13 represents the calculations of the sonic boom for the body N1 at various heat supply near the body. On can see at the abscissa axis the relative value C_x / C_x^1, where C_x is wave drag coefficient of a body if there any source of heat, C_x^1 is wave drag coefficient of the body N1 without any source of heat. The ordinate axis the sonic boom level is shown.

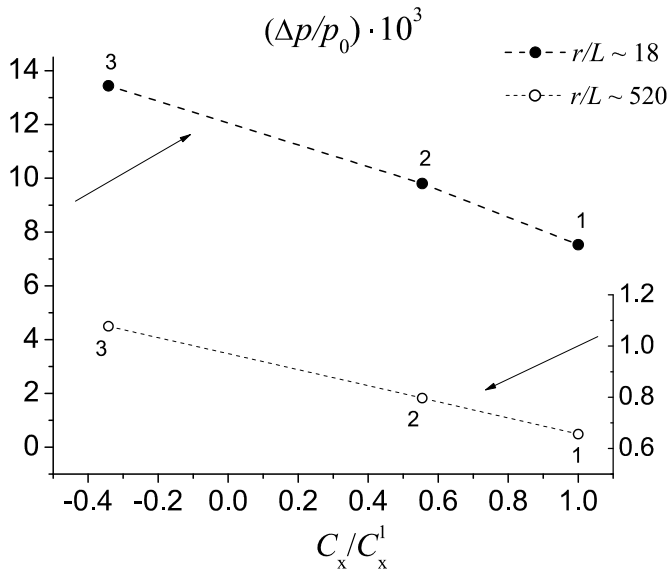

Fig. 13. Influence of heat supply to the gas on the drag coefficient and intensity of shock waves.

1 – T/T_0 = 1; *2* – T/T_0 = 1.123; *3* – T/T_0 = 1.4.

The points *1*, *2* and *3* indicate the levels of sonic boom at T/T_0 = 1, T/T_0 = 1.123, T/T_0 = 1.4. One can see that supplying energy to the external gas flow allows reducing the wave drag coefficient of the body, but it does not insure reducing of the sonic boom. In reverse supplying additional energy to the gas flow can results by increase of the sonic boom. In case of negative values of the wave drag coefficient the maximum values of the sonic boom level can be reached.

The work showed the possibility to apply the "phantom bodies" method for calculating shock waves parameters at long distances from the body. Comparing with calculation results done by means of other methods showed high accuracy of the "phantom bodies" method. One applied this method to calculate the sonic boom from

various thin axisymmetric bodies within the models of viscous and non-viscous gas applied for calculating the flow in the near and mean field. It is shown that the gas viscosity can be neglected in calculations of sonic boom because the viscosity influence manifests only in calculations of tails shock wave intensity in the near field. We confirmed the result obtained before by other authors about the minimal sonic boom for thin bodies with minimal coefficient of wave drag. It is shown that for nonhomogeneous gas in case of energy supply to the external flow one can obtain increasing of the sonic boom at lowering the wave drag coefficient.

REFERENCES

1. **Potapkin A.V., Yudintsev Y.N.** Numerical solution of the problem about focusing shock waves formed by a supersonic aircraft. // Uch. Zap. TsAGI. 1983. Vol. XIV, No. 4. P. 26–36.
2. **Chirkashenko V.F., Yudintsev Y.N.** The parameters of the shock waves from axisymmetric bodies in homogeneous atmosphere // Proc. SB AS USSR Technical science series. 1984. Ed. 3. P. 16–21.
3. **Kovalenko V.V., Chernyshev S.L.** About the question of sonic boom reducing // Uch. Zap. TsAGI. 2006. Vol. XXXVII, No. 3. P. 53–63.
4. **Potapkin A.V., Korotaeva T.A., Moskvichev D.Yu., Shashkin A.P., Maslov A.A., Silkey J.S., Roos F.W.** An advanced approach for the far-field sonic boom prediction: AIAA Paper 2009-1056. 2009.
5. **Potapkin A.V., Moskvichev D.Yu.** Calculation of shock-wave parameters far from origination by combined numerical-analytical methods // J. Appl. Mech. Tech. Phys. 2011. Vol. 52, No. 2. P. 169–177.
6. **Pyhmid I. I.** The Supersonic Boom of a Projectile Related to Drag and Volume // J. Aero. Sci. 1961. Vol. 28.
7. **Whitham G.B.** The flow pattern of a supersonic projectile // Comm. Pure Appl. Math. 1952. Vol. 5, No. 3. P. 301-348.
8. **Landau L.D.** About shock waves at long distances from their generating area // J. Appl. Math. Mech. 1945. Vol. IX, No. 4, P. 286–292.
9. **Hayes W.D., Haefeli R.C., Kulsrud H.E.** Sonic boom propagation in a stratified atmosphere, with computer program: NASA CR – 1299, 1969.
10. **Godunov S.K. et al.** The numerical solution of multi-dimensional problems of gas dynamics. Moscow: Nauka, 1976.